Drag Measurements on a Laminar Flow Body of Revolution

David A. Dress*
NASA Langley Research Center, Hampton, Virginia

Abstract

LOW-SPEED wind-tunnel drag force measurements were taken on a laminar flow body of revolution free of support interference. This body was tested at zero incidence in the NASA Langley 13 in. Magnetic Suspension and Balance System (MSBS). The primary objective of these tests was to determine the drag force measuring capabilities of the 13 in. MSBS. The drag force calibrations and wind-on repeatability data let us assess these capabilities. Other studies included the effects of fixing transition and surface flow visualizations using both liquid crystals and oil flow. In addition, the drag coefficient data from this study are compared with data from another source.

Contents

Background

Support interference is a serious problem in testing models in wind tunnels.[1,2] Using a Magnetic Suspension and Balance System (MSBS)[3] is the only way to eliminate completely support interference. With the elimination of the support, not only will the flow distortion produced by the sting be eliminated, but many other advantages will accrue, such as 1) elimination of model modifications to accomodate the sting, 2) ease of model movement for dynamic testing, 3) fast, efficient testing at any attitude, and 4) improvement in productivity due to elimination of stings and struts.

Since the late 1970's, in-house activity with MSBS's has steadily increased at NASA Langley. Most of the effort has been aimed at improving the 13 in. MSBS by using a digital control system and an optical position sensing system. However, in 1984 this MSBS was combined with a small low-speed ($M \leq 0.5$) wind tunnel, and in 1986 a program was initiated to obtain drag data on various axisymmetric shapes at zero incidence. The results reported here are part of this program.

Description of Model

The profile of the laminar flow body (see Fig. 3) was generated from an eight-parameter class of rounded-nose, tailboom bodies described in Ref. 4. This class of bodies was developed to verify a method of shaping axisymmetric bodies to produce minimum drag in incompressible, nonseparating flow at zero incidence. The model used in this study is 12 in. long with a fineness ratio of 7.5.

Drag Force Characteristics and Repeatability of Data

A drag force calibration was performed with a full-scale load of 242.5 gf. The data was fitted with a second-order polynomial. The rms of the errors between the applied loads and the calculated loads from the polynomial equation is 0.27 gf or 0.11% of the full-scale calibration load.

Wind-on drag force measurements were taken for this body over the Mach number range from approximately 0.05 to 0.2. The results, presented in Fig. 1, indicate that the drag coefficient $C_{D,\text{wet}}$ (based on wetted surface area) decreases as the length Reynolds number R_L increases. This figure also shows a repeat run comparison; there is excellent repeatability of the data. The rms of the differences between the first and second runs in terms of drag force is approximately 1.4 gf or 0.58% of the maximum calibration load of 242.5 gf.

Figure 2 is an oil flow photograph from the present study showing a laminar separation bubble at $R_L = 1.2 \times 10^6$. Figure 3 is a liquid crystal[5] flow visualization photograph also showing this laminar separation region at the same R_L. (Note that Fig. 3 was artificially enhanced to highlight the "colored" regions on the model. This was necessary due to poor contrast on the original photograph.) A laminar separation line and turbulent reattachment line are shown in both figures. At lower values of R_L it was observed that the separation line was at a more forward station on the body. It is estimated that this separation line originated between $x/L = 0.50$ and $x/L = 0.55$. This separation line moved rearward as R_L increased. It also was observed that the reattachment line originated near the tail of the body at a lower R_L. This reattachment line

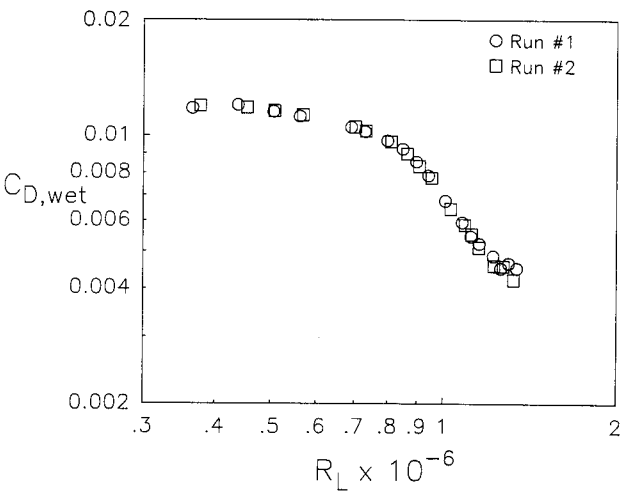

Fig. 1 Repeatability of drag characteristics of laminar flow body.

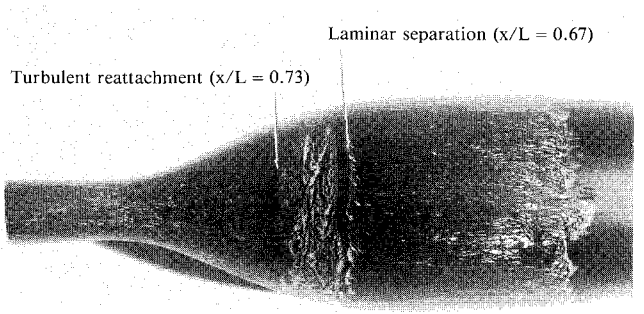

Fig. 2 Photograph of oil flow visualization. Free transition. $R_L = 1.2 \times 10^6$.

Received May 12, 1988; presented as paper 88-2010 at the AIAA 15th Aerodynamic Testing Conference, San Diego, CA, May 18-20, 1988; synoptic received Dec. 22, 1988. Full paper available at AIAA Library, 555 W. 57th St., New York, NY 10019. Price: microfiche, $4.00; hard copy, $9.00. **Remittance must accompany order.**

*Research Engineer. Member AIAA.

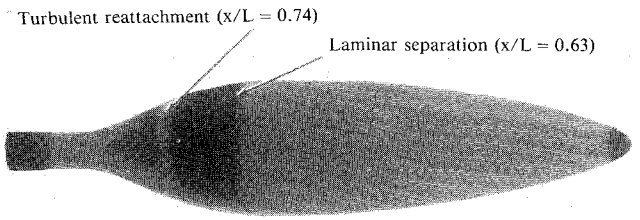

Fig. 3 Photograph of liquid crystal flow visualization. Free transition. $R_L = 1.2 \times 10^6$.

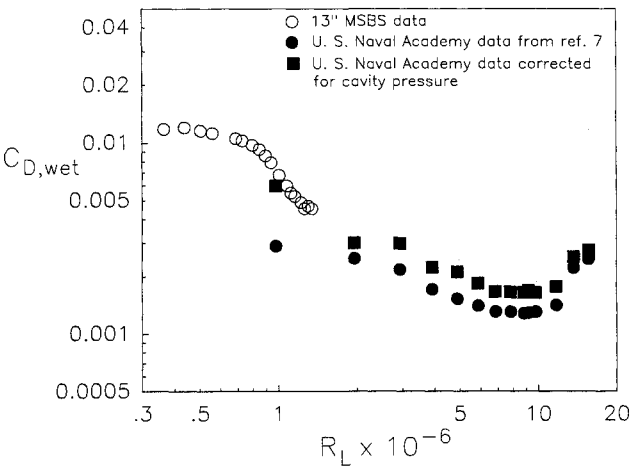

Fig. 4 Comparison of drag characteristics with U.S. Naval Academy data.

moved forward as R_L increased. Thus, this separation bubble decreased in size as R_L increased.

Comparison with Other Data

A sting-mounted version of this shape also was tested at the United States Naval Academy.[6,7] Only one data point from this study overlaps the data from Ref. 7. However, the data is compared by looking at the relative drag coefficient levels as shown in Fig. 4. The tabular data from Ref. 7 was used for this comparison. There is a large discrepancy in $C_{D,wet}$ at $R_L = 1 \times 10^6$ when comparing the uncorrected Naval Academy data with the data from the present study. This author subsequently corrected the Naval Academy data for cavity pressure using pressure measurements given in Ref. 7. As shown in Fig. 4, the corrected data are in good agreement with the results from the present study. The author attributes the difference that still exists at $R_L = 1 \times 10^6$ to one or more of the following:

1) The sting at the rear of the model used at the Naval Academy may act as an extension of the body. This would result in a higher fineness ratio shape, which would reduce the overall drag coefficient.

2) The sting would divide and alter the wake region at the tail of the model, possibly reducing the overall drag.

3) The rear portion of the model used at the Naval Academy was slightly modified to accommodate the sting. This model does not have the slight flair at the tail as in the case of the 13 in. MSBS model. This slight modification may have altered the wake pattern.

Drag coefficient data on this laminar-flow body are also presented in Ref. 6. However, these drag coefficients do not agree with those in Ref. 7. The differences currently are not understood.

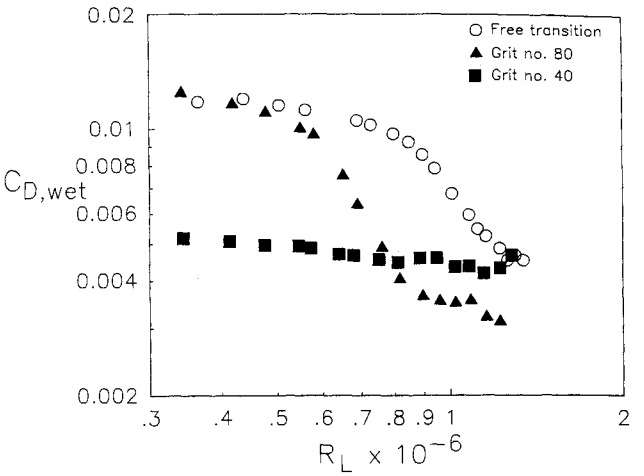

Fig. 5 Drag characteristics of laminar flow body. Comparison of fixed and free transition. Fixed at 50% station with both number 80 grit and number 40 grit.

Comparison of Free and Fixed Transition

Several fixed transition runs at different model stations were performed in an effort to assess the effect of fixing transition on the laminar separation bubble. Three-dimensional abrasive grain transition grit was used. One set of runs involved fixing transition at the 50% station using grit numbers 80 and 40. These correspond to nominal trip sizes of 0.008 and 0.020 in., respectively. Transition was fixed at this location to retain a large portion of laminar flow while avoiding laminar separation by making the boundary layer turbulent just ahead of the separation bubble. Figure 5 shows a free and fixed transition comparison. The smaller grit (number 80) did not trip the boundary layer to fully turbulent flow until $R_L = 1 \times 10^6$. The larger grit appears to have effectively tripped the boundary length through the entire Reynolds number range. In fact, at Reynolds numbers above 8×10^5, the boundary layer has thinned to the point where the number-40 grit is too large. This results in grit drag for Reynolds numbers greater than 8×10^5, where $C_{D,wet}$ is larger for the number-40 grit data as compared to the number-80 grit data.

References

[1]Tuttle, M. H. and Gloss, B. B., "Support Interference of Wind Tunnel Models—A Selective Annotated Bibliography," NASA TM-81909, March 1981.

[2]Tuttle, M. H. and Lawing, P. L., "Support Interference of Wind Tunnel Models—A Selective Annotated Bibliography," Supplement to NASA TM-81909, May 1984.

[3]Tuttle, M. H., Kilgore, R.A., and Boyden, R. P., "Magnetic Suspension and Balance Systems—A Selected, Annotated Bibliography," NASA TM-84661, July 1983.

[4]Parsons, J. S., Goodson, R. E., and Goldschmied, F. R., "Shaping of Axisymmetric Bodies for Minimum Drag in Incompressible Flow," *Journal of Hydronautics,* Vol. 8, No. 3, 1974, pp. 100–107.

[5]Holmes, B. J. and Obara, C. J., "Advances in Flow Visualization Using Liquid-Crystal Coatings," Society of Automotive Engineers, Warrendale, PA, SAE TP-871017, April 1987.

[6]Hansen, R. J. and Hoyt, J. G., "Laminar-To-Turbulent Transition on a Body of Revolution With an Extended Favorable Pressure Gradient Forebody," *Journal of Fluids Engineering,* Vol. 106, June 1984, pp. 202–210.

[7]Hoyt, J. G., III, "Preliminary Resistance Test of Laminar Flow Submersible," U.S. Naval Academy, Hydromechanics Laboratory, Annapolis, MD, USNA HL-88-6, Dec. 1988.